

V_{cs} from Pure Leptonic Decays of D_s with Radiative Corrections

Guo-Li Wang^{a,c}, Tai-Fu Feng^{b,c} and Chao-Hsi Chang^c

February 1, 2019

^a, Department of Physics, FuJian Normal University, FuZhou 350007, China

^b, Department of Physics, NanKai University, TianJin 300070, China

^c, Institute of Theoretical Physics, Academia Sinica, P.O.Box 2735, BeiJing 100080, China

Abstract

The radiative corrections to the pure leptonic decay $D_s \rightarrow \ell \nu_\ell$ up-to one-loop order is presented. We find the virtual photon loop corrections to $D_s \rightarrow \tau \nu_\tau$ is negative and the corresponding branching ratio is larger than 3.51×10^{-3} . Considering the possible experimental resolutions, our prediction of the radiative decay $D_s \rightarrow \tau \nu_\tau \gamma$ is not so large as others, and the best channel to determine the V_{cs} or f_{D_s} is $D_s \rightarrow \mu \nu_\mu \gamma$.

PACS numbers: **13.20.Fc**, **12.39.Jh**, **13.40.Ks**

The pure-leptonic decay $D_s \rightarrow \ell \nu_\ell$ (see, Fig.1) can be used to determine the decay constant f_{D_s} if the fundamental Cabibbo-Kobayashi-Maskawa matrix element V_{cs} of Standard Model (SM) is known. Conversely if we know the value of decay constant f_{D_s} from other method [1, 2, 3], these process also can be used to extract the matrix element V_{cs} . But there are the well known effect of helicity suppression we can see it by factor of $m_\ell^2/m_{D_s}^2$:

$$\Gamma(D_s \rightarrow \ell \bar{\nu}_\ell) = \frac{G_F^2}{8\pi} |V_{cs}|^2 f_{D_s}^2 m_{D_s}^3 \frac{m_\ell^2}{m_{D_s}^2} \left(1 - \frac{m_\ell^2}{m_{D_s}^2}\right)^2, \quad (1)$$

Of them only the process $D_s \rightarrow \tau \nu_\tau$ is special, it does not suffer so much from the helicity suppression, and its branching ratio may reach to 4.5% in SM. However the produced τ will decay promptly and one more neutrino is generated in the cascade decay at least, thus it makes the decay channel difficult to be observed. For the channels $D_s \rightarrow e \nu_e$ and $D_s \rightarrow \mu \nu_\mu$, besides the small branching ratios, there are only one detected final state, the measurement of such channels are very difficult.

Fortunately, having an extra real photon emitted in the leptonic decays, the radiative pure leptonic decays can escape from the suppression [4, 5, 6], furthermore, as pointed out in Ref.[7], with the extra photon to identify the decaying pseudoscalar meson D_s in experiment from the backgrounds has advantages, since one more particle can be detected in the detector. Although

the radiative corrections are suppressed by an extra electromagnetic coupling constant α , it will not be suppressed by the helicity suppression. Therefore, the radiative decay may be comparable, even larger than the corresponding pure leptonic decays[4, 5, 6].

The radiative pure leptonic decays, theoretically, have infrared divergences and will be canceled with those from loop corrections of the pure leptonic decays. In all the existing calculation of radiative decays[4, 5, 6], this part is ignored, since they do not include the radiative corrections of the pure leptonic decays. In this paper, we are interested in considering the radiative decays and the pure leptonic decays with one-loop radiative corrections together. Since the process $D_s \rightarrow \tau \nu_\tau$ does not suffer the helicity suppression and has a large branching ratio, the corresponding loop correction (virtual photon) to these process should have a considerable larger branching ratio, at least comparing with the radiative decay, and can not be ignored.

The contributions of the radiative decays are corresponding to the four diagrams in Fig.2. According to the constituent quark model which is formulated by Bethe-Salpeter (B.-S.) equation, the amplitude turns out to be the four terms $M_i (i = 1, 2, 3, 4)$:

$$M_1 = Tr \left[\int \frac{d^4 q}{(2\pi)^4} \chi(p, q) i \left(\frac{G_F m_w^2}{\sqrt{2}} \right)^{\frac{1}{2}} \gamma_\mu (1 - \gamma_5) V_{cs} \right] \times$$

$$\frac{i \left(-g^{\mu\nu} + \frac{p^\mu p^\nu}{m_w^2} \right)}{p^2 - m_w^2} i e [(p' + p)_\lambda g_{\nu\rho} + (k - p')_\nu g_{\rho\lambda} + (-p - k)_\rho g_{\nu\lambda}] \epsilon^\lambda \times$$

$$\frac{i \left(-g^{\rho\sigma} + \frac{(p-k)^\rho (p-k)^\sigma}{m_w^2} \right)}{(p-k)^2 - m_w^2} \bar{\ell} \frac{ig}{2\sqrt{2}} \gamma_\sigma (1 - \gamma_5) \nu_\ell, \quad (2)$$

$$M_2 = Tr \left[\int \frac{d^4 q}{(2\pi)^4} \chi(p, q) i \left(\frac{G_F m_w^2}{\sqrt{2}} \right)^{\frac{1}{2}} \gamma_\mu (1 - \gamma_5) V_{cs} \right] \frac{i \left(-g^{\mu\nu} + \frac{p^\mu p^\nu}{m_w^2} \right)}{p^2 - m_w^2}$$

$$\times \bar{\ell} (-ie) \not{\epsilon} \frac{i}{\not{k}_\ell - m_\ell} \frac{ig}{2\sqrt{2}} \gamma_\nu (1 - \gamma_5) \nu_\ell, \quad (3)$$

$$M_3 = Tr \left[\int \frac{d^4 q}{(2\pi)^4} \chi(p, q) i \left(\frac{G_F m_w^2}{\sqrt{2}} \right)^{\frac{1}{2}} \gamma_\mu (1 - \gamma_5) V_{cs} \frac{i}{\frac{m_s}{m_s + m_c} \not{p} + \not{q} - \not{k} - m_s} \left(-i \frac{e}{3} \not{\epsilon} \right) \right]$$

$$\times \frac{i \left(-g^{\mu\sigma} + \frac{(p-k)^\mu (p-k)^\sigma}{m_w^2} \right)}{(p-k)^2 - m_w^2} \bar{\ell} \frac{ig}{2\sqrt{2}} \gamma_\sigma (1 - \gamma_5) \nu_\ell, \quad (4)$$

$$M_4 = Tr \left[\int \frac{d^4 q}{(2\pi)^4} \chi(p, q) \left(i \frac{2e}{3} \not{\epsilon} \right) \frac{i}{-(\frac{m_c}{m_s + m_c} \not{p} - \not{q} - \not{k}) - m_c} i \left(\frac{G_F m_w^2}{\sqrt{2}} \right)^{\frac{1}{2}} \gamma_\mu (1 - \gamma_5) V_{cs} \right]$$

$$\times \frac{i \left(-g^{\mu\sigma} + \frac{(p-k)^\mu (p-k)^\sigma}{m_w^2} \right)}{(p-k)^2 - m_w^2} \bar{\ell} \frac{ig}{2\sqrt{2}} \gamma_\sigma (1 - \gamma_5) \nu_\ell, \quad (5)$$

where $\chi(p, q)$ is Bethe-Salpeter wave function of the meson D_s ; p is the momentum of D_s ; ϵ , k are the polarization vector and momentum of the emitted photon.

As the D_s meson is a nonrelativistic S-wave bound state in nature, higher order relativistic corrections may be small, being the first order approximation for a S-wave state, we ignore q dependence in amplitude and in the D_s wave-function and write the wave function of the meson D_s as:

$$\int \frac{d^4 q}{(2\pi)^4} \chi(p, q) = \frac{\gamma_5(\not{p} + m)}{2\sqrt{m}} \psi(0).$$

Here $\psi(0)$ is the wave function at origin in the coordinate space, and by definitions it connects to the decay constant f_{D_s} :

$$\psi(0) = 2\sqrt{m} f_{D_s},$$

where m is the mass of D_s meson. Moreover we note that for convenience we take unitary gauge for weak boson to do the calculations throughout the paper.

There is infrared infinity when performing phase space integral about the square of matrix element at the soft photon limit. It is known that the infrared infinity can be cancelled completely by that of the loop corrections to the corresponding pure leptonic decay $D_s \rightarrow \ell \nu$.

If Feynman gauge for photon is taken, the amplitude of loop corrections corresponding to the box diagrams (a), (b) of Fig.3.1 can be written as:

$$M_{(2)}(a) = \frac{2}{3} e A \int \frac{d^4 l}{(2\pi)^4} \left[\frac{-4i\varepsilon^{\alpha\mu\beta\nu} p_\alpha l_\beta - 4(p_\mu l_\nu - p \cdot l g_{\mu\nu} + p_\nu l_\mu) + \frac{8m_c}{m_s + m_c} p_\mu p_\nu}{l^2(l^2 - 2p \cdot l - m_w^2)(l^2 - \frac{2m_c}{m_s + m_c} p \cdot l)[l^2 - 2l \cdot (p - k_2)]} \right] \\ \times \bar{\ell} [2(p - k_2)_\mu - \gamma_\mu \not{l}] (-\gamma_\nu) (1 - \gamma_5) \nu_\ell, \quad (6)$$

$$M_{(2)}(b) = -\frac{1}{3} e A \int \frac{d^4 l}{(2\pi)^4} \left[\frac{-4i\varepsilon^{\alpha\mu\beta\nu} p_\alpha l_\beta + 4(p_\mu l_\nu - p \cdot l g_{\mu\nu} + p_\nu l_\mu) - \frac{8m_s}{m_s + m_c} p_\mu p_\nu}{l^2(l^2 - 2p \cdot l - m_w^2)(l^2 - \frac{2m_s}{m_s + m_c} p \cdot l)[l^2 - 2l \cdot (p - k_2)]} \right] \\ \times \bar{\ell} [2(p - k_2)_\mu - \gamma_\mu \not{l}] (-\gamma_\nu) (1 - \gamma_5) \nu_\ell, \quad (7)$$

where the l , k_2 denote the momenta of the loop and the neutrino respectively. These two terms also have infrared infinity when integrating out the loop momentum l .

After doing the on-mass-shell subtraction, the terms corresponding to vertex and self-energy diagrams (c), (d), (e), (f) of Fig.3.2 can be written as:

$$M_{(2)}(c + d + e + f) = \frac{ieA}{4\pi^2} \bar{\ell} \not{p} (1 - \gamma_5) \nu_\ell \times \left[\ln(4) - \frac{8}{9} + \frac{2}{9} \frac{m_s - m_c}{m_s + m_c} \ln\left(\frac{m_s}{m_c}\right) \right. \\ \left. + \left(\frac{2}{9} + \frac{8}{9} \frac{m_c}{m_s + m_c}\right) \ln\left(\frac{m_s + m_c}{m_s}\right) + \left(\frac{8}{9} + \frac{8}{9} \frac{m_c}{m_s + m_c}\right) \ln\left(\frac{m_s + m_c}{m_c}\right) \right. \\ \left. + \frac{2}{\varepsilon_I} - 2\gamma + \ln\left(\frac{4\pi\mu^2}{m^2}\right) + \ln\left(\frac{4\pi\mu^2}{m_e^2}\right) \right]. \quad (8)$$

where A is:

$$A = \frac{f_{D_s} \left(\frac{G_F m_w^2}{\sqrt{2}}\right)^{\frac{1}{2}} V_{cs} e g}{2\sqrt{2}} = f_{D_s} \left(\frac{G_F m_w^2}{\sqrt{2}}\right) V_{cs} e.$$

The other loop diagrams (we do not show them) always have a further suppression factor m^2/m_w^2 to compare with the loop diagrams in Fig.3, and there is no infrared infinity in these

loop diagrams, we can ignore their contributions safely. Furthermore we should note that in our calculations throughout the paper, the dimensional regularization to regularize both infrared and ultraviolet divergences is adopted, while the on-mass-shell renormalization for the ultraviolet divergence is used.

Detail cancellation of infrared divergence is given in Ref[8]. Here we simply show the results. The ‘whole’ leptonic decay branching ratios, i.e., the sum of the corresponding radiative decay branching ratios and the corresponding pure leptonic decay branching ratios with radiative corrections, and put them in Table (1). The reason we put the radiative decay and the pure leptonic decay with radiative corrections together is to make the branching ratios not to depend on the experimental resolution for a soft photon. For comparison, the branching ratios of each pure leptonic decay at tree level is also put in Table (1). The values for the parameters $\alpha = 1/132$, $|V_{cs}| = 0.974$ [9], $m_{D_s} = 1.9686$ GeV, $m_s = 0.5$ GeV, $m_c = 1.7$ GeV, $f_{D_s} = 0.24$ GeV[10] and the lifetime $\tau(D_s) = 0.469 \times 10^{-12}$ s[9].

Table (1) Branching Ratios of the ‘Whole’ and Tree Level Leptonic Decays

	‘whole’	tree
$Br_e(10^{-5})$	2.56	0.0108
$Br_\mu(10^{-3})$	4.706	4.605
$Br_\tau(10^{-2})$	4.138	4.489

We can see that, the ‘whole’ decay branching ratios Br_e and Br_μ are larger than the corresponding branching ratios of tree level, while the ‘whole’ Br_τ is smaller than the tree level one. It means the contributions of loop corrections are negative, the dominate contributions of first order corrections to the pure leptonic D_s decays are radiative decays when the lepton is e or μ , and is loop corrections when the lepton is τ . So, the loop contributions are important for the decays $D_s \rightarrow \mu\nu_\mu$ and $D_s \rightarrow \tau\nu_\tau$, especially for the later. Through Table (1), we obtained that the radiative decay has a branching ratio $Br(D_s \rightarrow \mu\nu_\mu\gamma) > 1.01 \times 10^{-4}$ and the loop correction to $D_s \rightarrow \tau\nu_\tau$ has a branching ratio $Br > 3.51 \times 10^{-3}$.

To see the contributions of the radiative decays precisely we present the radiative decay branching ratios with a cut of the photon energy, i.e., the branching ratios of the radiative decays $D_s \rightarrow l\nu\gamma$ with the photon energy $E_\gamma \geq k_{min}$ as the follows: $k_{min} = 0.00001$ GeV, $k_{min} = 0.0001$ GeV, $k_{min} = 0.001$ GeV, $k_{min} = 0.01$ GeV and $k_{min} = 0.1$ GeV respectively in Table (2). We also show the existing results of other methods in the same table.

Table (2): The Radiative Decay branching ratios with cuts of the photon momentum and the results of Ref[4, 5, 6]

k_{min}	Br_e	Br_μ	Br_τ
GeV	10^{-5}	10^{-4}	10^{-6}
0.00001	2.552	4.901	6.336
0.0001	2.552	3.908	4.597
0.001	2.551	2.915	2.868
0.01	2.549	1.927	1.217
0.1	2.475	0.971	0.727
Ref[4]	10	1	—
Ref[5]	17	1.7	—
Ref[6]	7.7	2.6	320

Figure 1: **Tree diagram for $D_s \longrightarrow \ell \nu_\ell$.**

Considering the possible experimental resolutions of photon, our prediction of the radiative decay branching ratios $Br(D_s \rightarrow e \nu_e \gamma)$ and $Br(D_s \rightarrow \mu \nu_\mu \gamma)$ are close to the values in Ref[4, 5, 6], but our prediction of $Br(D_s \rightarrow \tau \nu_\tau \gamma)$ is much smaller than the one in Ref[6]. In our model, if we using a smaller cut k_{min} , then obtained a larger $Br(D_s \rightarrow \ell \nu_\ell \gamma)$, because the decay widths depend on $Log(k_{min})$ [8], the change of branching ratios will be not so much on the selection of k_{min} , we can see this in Table (2), and for another example, if $k_{min} = 1.0 \times 10^{-10}$ GeV, then we obtain $Br(D_s \rightarrow e \nu_e \gamma) = 3.59 \times 10^{-5}$, $Br(D_s \rightarrow \mu \nu_\mu \gamma) = 1.38 \times 10^{-3}$, $Br(D_s \rightarrow \tau \nu_\tau \gamma) = 2.11 \times 10^{-5}$, but so small a k_{min} , it is very difficult in experiment. We can conclude that the best radiative decay channel is easy to search in experiment is $D_s \rightarrow \mu \nu_\mu \gamma$.

For the convenience to compare with experiments, we present the photon spectrum of the radiative decays in Fig.4 and Fig.5. In addition, we should note that the widths are quite sensitive to the decay constant f_{D_s} , and are sensitive to the values of the quark masses m_s and m_c .

References

- [1] As.Abada et al., Nucl. Phys. B**376** (1992) 172.
- [2] C.R.Allton et al., APE Collaboration, Nucl. Phys. B(Proc. Suppl.)**34** (1993) 465.
- [3] C.W.Bernard et al., Phys. Rev. D**49** (1994) 2536.
- [4] Gustavo Burdman,T.Goldman and Daniel Wyler, Phys. Rev. D**51** (1995) 111.
- [5] D.Arwood, G.Eilam and A.Soni, Mod. Phys. Lett. A**11** (1996) 1061.
- [6] C.Q.Geng,C.C.Lih and Wei-Min Zhang, **hep-ph/0012066**.
- [7] C.-H. Chang, C-D Lü, G.-L. Wang and H.-S. Zong, Phys. Rev. D**60** (1999) 114013.
- [8] Guo-Li Wang et al., unpublished.
- [9] D.E.Groom et al., The European Physical Journal C**15** (2000) 1.
- [10] C.R.Allton et al., APE Collaboration, Nucl. Phys. B(Proc. Suppl.) **34** (1993) 456.

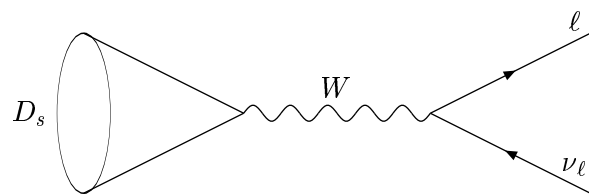
Figure 2: **Diagrams for $D_s \longrightarrow \ell \nu \gamma$.**

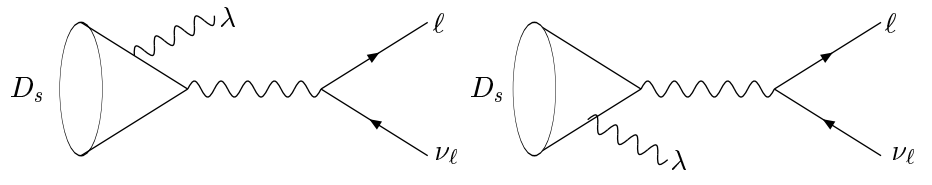
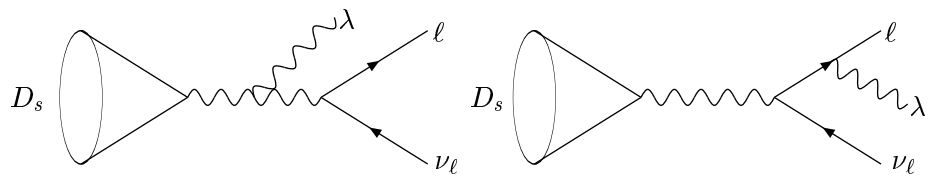
Figure 3: **1. Box-loop diagrams for $D_s \longrightarrow \ell \nu$.**

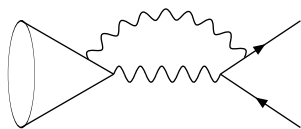
Figure 3: **2. Self-energy and vertex diagrams for $D_s \rightarrow \ell \nu$.**

Figure 4: **Photon energy spectra of radiative decays $D_s \longrightarrow \ell \nu_\ell \gamma$ ($\ell = e, \mu$).**

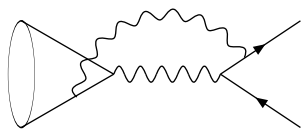
Figure 5: **Photon energy spectra of radiative decays $D_s \longrightarrow \tau \nu_\tau \gamma$.**



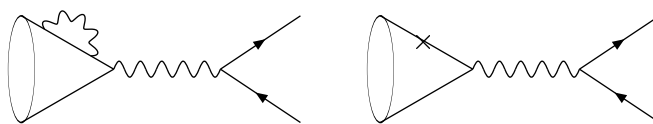




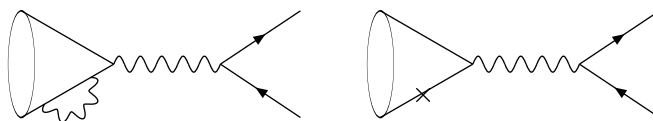
(a)



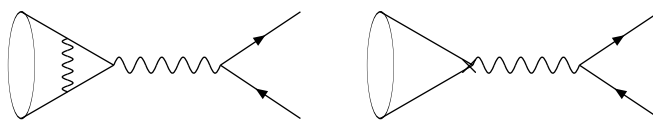
(b)



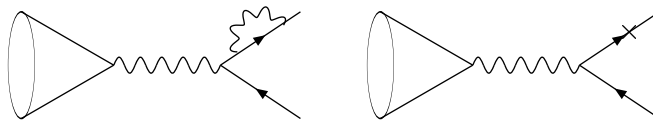
(c)



(d)



(e)



(f)

